Chapter Five: Atmospheric Processing of Organic Aerosols: Measurements at Urban, Rural and Remote Locations

5.1 Introduction

Understanding the composition of atmospheric aerosol particles is necessary for identifying their sources and predicting their effect on the various atmospheric processes discussed in the introduction (see section 1.1.2). Although organic compounds typically account for 10 − 70% of the total dry fine particle mass in the atmosphere [*Gray et al., 1986; Middlebrook et al., 1998*], organic PM concentrations, composition and formation mechanisms are not well understood, particularly in relation to the other major fine particle constituents, i.e. sulphate and nitrate compounds. This is because particulate organic matter is part of a complex atmospheric system with hundreds of different compounds, both natural and anthropogenic, covering a wide range of chemical and thermodynamic properties [*Saxena and Hildemann, 1996*]. The presence of semi-volatile compounds complicates the sampling of organic particulate matter. In addition, there is a current lack of a single technique that is capable of analysing the entire range of organics present.

Organic particulate matter is both emitted directly in particle form (primary organic aerosols) and formed in the atmosphere through photochemical oxidation of reactive organic gases forming low-volatility products that condense or adsorb onto particle surfaces, or absorb into pre-existing particulate matter resulting in the addition of material to atmospheric particles; this process is known as "secondary organic aerosol particle formation". Under certain conditions atmospheric reaction products can nucleate to form new particles. Both biogenic and anthropogenic sources contribute to primary and secondary organic particles [*Hildemann et al., 1996*]. Secondary organic particles can be a major contributor to fine particulate matter levels in both urban and rural atmospheres [*Turpin and Huntzicker, 1995; Castro et al., 1999*]. However, the contributions of the primary and secondary components of particulate organic carbon (OC) have long been difficult to quantify. The lack of a direct chemical analysis method for the identification of either of these components has led researchers to employ several indirect methods. These include the use of tracer compounds for either the primary or the secondary OC [*Gray et al., 1986; Turpin and Huntzicker, 1991*], the use

of models describing the formation of secondary OC [*Pandis et al., 1992*] and the use of models describing the emission and dispersion of primary OC [*Harley and Cass, 1995*].

One of the main objectives of this work has been to validate the AMS as a tool of quantitative measurement of the size distribution and chemical composition of the non-refractory fraction of submicron atmospheric particles ($\sim PM_{1.0}$) and utilise it, in conjunction with other instruments, to further our current understanding of the behaviour of atmospheric aerosols. The AMS has been deployed in many field studies covering a wide range of environments worldwide over the past few years. In this chapter, data from locations representing various environments have been synthesised in order to investigate and improve our understanding of the sources, distribution, chemical composition and processing of atmospheric particles, in particular its organic fraction. Specifically, the aim of this chapter is to characterise the variability of the organic particulate composition and size distributions as a function of location and photochemical activity using, mainly, AMS data representing a range of emission-dominated to formation-controlled regimes in different parts of the world, and investigate the effect of atmospheric processing on the chemical composition and size distribution of the organic fraction. Correlations with gas phase marker compounds have been used to explain both sources and modal behaviour of organic particulate. Identification of organic ion series, as well as key mass fragments has been used in an attempt to further understand the chemical composition of the organic fraction of the aerosol particles.

The data discussed in this chapter have been collected in urban locations in Manchester and Edinburgh in the UK and Vancouver in Canada. Two data sets have been obtained in Manchester during summer and winter periods. On the other hand, data from rural and semi-rural locations in Canada, a high alpine site in central Europe and a remote marine site on Jeju Island, South Korea have also been obtained. It is important to note that there is no intention in this chapter to provide a detailed analysis of the individual field studies. Such data have been already presented for the two U.K. cities by *Allan et al.*, [*2003a; 2003b*], for the Korean data by *Topping et al.*, [*2004*], and the Canadian data by *Alfarra et al.*, [*2004*] and *Boudries et al.*, [*2004*]. The reader is directed to these

publications for more background details on the corresponding experiments and a more detailed discussion of the sources, composition and behaviour of the inorganic fraction of the aerosols. A detailed discussion of the data from the high alpine location is presented in Chapter 7 of this thesis. All sampling locations and protocols are briefly described in the following section.

5.2 Field Sites and AMS Sampling

5.2.1 Edinburgh, UK *(2000)*

The first field deployment of the UMIST AMS was during the third campaign of the *Sources And Sinks of Urban Aerosol (SASUA3)* experiment in Edinburgh, UK in October- November 2000. The experiment was organised jointly between the Centre for Ecology and Hydrology (CEH) in Edinburgh and UMIST, with the aim of measuring aerosol fluxes and emission velocities above the city. The AMS involvement in this experiment was mainly a chance to provide a first shakedown for the UMIST instrument and to validate that it is capable of producing reliable and robust field data. The simultaneous aerosol size and chemical composition measurements made by both CEH and UMIST groups provided a good chance for data comparisons with the AMS [*Allan et al., 2003a*].

AMS Measurements were made at the Observatory House on the top of Calton Hill (55.955 °N, 3.184 °W), 50 m above the main street in the centre of the city of Edinburgh from 31/10 to 10/11/2000, with an averaging time of 30 min. A basic inlet, made of a gauze-covered, upturned funnel at the end of 2-m long 6.35 mm internal diameter tube, was used for sampling. The suspected major local particle source was Princess Street, the main shopping street in the centre of Edinburgh with a high traffic density. *Dorsey et al.*, [*2002*] provides a more detailed description of the site and the SASUA project.

5.2.2 Jeju Island, South Korea *(2001)*

ACE-Asia was the third of the *Aerosol Characterisation Experiments* (ACE) organised by the International Global Atmospheric Chemistry Project (IGAC). The experiment was a major international collaboration led by the National Science Foundation (NSF)

and National Oceanic and Atmospheric Administration (NOAA) in the USA. It took place on the South Korean island of Jeju and was designed to study the size and chemical composition along with other radiative properties of the Asian aerosols in order to establish a better understanding of their radiative impact in the atmosphere [*Huebert et al., 2003*].

The island of Jeju is a major resort with no large industrial sources [*Carmichael et al., 1997*]. It is located in the Yellow Sea about 100 km to the south of the Korean mainland, 500 km to the northeast of Shangahi, China, and 250 km to the west of Kyushu Island, Japan. Its location and lack of major local sources of pollution make Jeju Island an ideal position to monitor the pollution in East Asia [*Carmichael et al., 1996; Carmichael et al., 1997; Chen et al., 1997*]. During ACE Asia, the AMS was deployed at the Gosan supersite (33.29 °N, 126.16 °E), located at the small costal village of Gosan on the western tip of Jeju Island overlooking the Yellow Sea. Measurements were made from 12/04 to 30/04/2001, with 30 min averaging time. The AMS sample flow was sub-sampled from a 10.5 m mast equipped with a standard PM_{10} inlet.

5.2.3 Manchester, UK *(2001 & 2002)*

AMS measurements have been carried out in Manchester during two periods in summer 2001, and winter 2002 with the aim of comparing the summer and winter aerosol composition and size distribution in Manchester, UK. During both periods, ambient aerosols were sampled through a standard PM_{10} inlet on the roof of the UMIST Main Building, approximately 30 m above street level and located near the centre of the city of Manchester (53.476 °N, 2.234 °W). The inlet was approximately 2 m above roof level and was connected to the AMS by a 25.4 mm internal diameter stainless steel tube approximately 7 m long. The nominal inlet flow rate was 17 l min^{-1} and the AMS sampled through a 2.8 mm internal diameter stainless steel tube. Gas phase measurements were carried out at 25 m above street level by an automated monitoring site (Department of the Environment, Transport and the Regions) on the roof of Manchester Town Hall, located about 0.75 km away in the centre of Manchester.

Summer Sampling took place between 14/06 and 25/06/2001, with 30 min averaging time, and winter measurements were taken between 17/01 and 28/01/2002.

5.2.4 British Columbia, Canada *(2001)*

In August 2001, the PACIFIC 2001 field study was conducted in the Lower Fraser Valley (LFV), British Columbia, Canada in order to provide a better understanding of the sources, formation and distribution of particulate matter and ozone in that area. The LFV has topographic features similar to that of the Los Angeles basin and experiences the interaction of urban, suburban, marine, and agricultural emissions of pollutants and their subsequent transformation in ambient air [*Li, 2004*]. The valley periodically experiences episodes of elevated levels of ozone and fine particulate matter in the summer resulting in poor visibility and possible health effects. These episodes are typically experienced when the region is under the influence of synoptic high pressure systems that lead to subsidence inversions which trap the surface primary pollutants in a shallow boundary layer [*Li et al., 1997*]. Specific goals of the PACIFIC 2001 study were to determine the horizontal and vertical distributions and physical and chemical characteristics of fine PM and ozone in order to understand the transition between primary emission and secondary aerosol formation in the valley, and to identify the major physical and chemical processes and roles of biogenic and anthropogenic emissions in the secondary organic aerosol particles and ozone formation [*Li, 2004*].

Two Aerodyne Aerosol Mass Spectrometers were operated at three main field sites during the PACIFIC 2001 experiment in the Lower Fraser Valley, British Columbia, Canada during the summer of 2001. The *Slocan Park* site was located in the city of Vancouver (49.244 ^{o}N, 123.049 ^{o}W) and represented a background urban location, where a mixture of primary and secondary particulate matter was expected. The site was surrounded by 2-3 storied residential houses situated at least 80 m away from the sampling location. There were no major point sources within a radius of 3 km of the site. Traffic in the nearby streets was typically light. The first AMS was deployed at this site from the 12/08 to 24/08/2001, and data was averaged every 15 min. Sampling was carried out through a $PM_{2.5}$ cyclone inlet about 2 m above the trailer roof using 8 m of 0.5" (1.27 cm) O.D. copper tubing, at a flow rate of 10 l min^{-1}. The *Langley site* was

selected to study the transition from an urban to rural setting, and to characterise particles arising from agricultural activities. It was located in the middle of agricultural fields to the southeast of the city of Vancouver (49.028 ^{o}N, 122.604 ^{o}W) with no nearby major residential houses or traffic. The second AMS was deployed at this site for the duration of the field study from the 12/08 to 01/09/2001, and collected data with 15 min averaging time. Ambient sampling was carried out using the same inlet system as the one described above for the Slocan Park site. The *Sumas mountain site* was located on the eastern side of the valley (49.052 ^{o}N, 122.246 ^{o}W). It was chosen to address the interaction between aging urban pollution and biogenic emissions resulting from the coniferous tree covered slopes of the mountain. The first AMS was relocated from Slocan Park to Sumas on 25/08 and continued to measure at the latter site to 30/08/2001, with 5 min averaging time, using the same inlet system from the Slocan Park site. For additional details about the PACIFIC 2001 objectives and other scientific findings, the reader is directed to volume 38, issue 34 of Atmospheric Environment (November 2004), which is a special issue on this specific experiment.

5.2.5 Jungfraujoch, Switzerland *(2002)*

AMS measurements have been made as part of the second *Cloud and Aerosol Characterisation Experiment* (CLACE 2)*,* which took place at the Jungfraujoch high-alpine research station (46.33 ^{o}N, 7.59 ^{o}E, 3580 m asl) in the Swiss Alps during June – July 2002. The objectives of the CLACE 2 and detailed description of the sampling location, protocol and scientific findings can be found in Chapter 7 of this thesis. During summer, the site is often influenced in the early afternoon by the planetary boundary layer (PBL) through thermally driven aerosol transport, while at other times and seasons, free tropospheric conditions prevail. Results reported in this chapter were for aerosol particles sampled, with 6 min averaging time through an inlet heated to 25 ^{o}C in order to evaporate all activated cloud droplets at an early stage of the sampling process leaving the ambient aerosol, including the cloud droplet residuals, to pass through the inlet and be sampled.

5.2.6 AMS Particle Collection Efficiency (*CE*)

Previous field studies [*Drewnick et al., 2003*] have shown that particle mass is underestimated by the AMS for ammonium sulphate dominated aerosol by a factor of 2 (i.e. $CE_{sulphate}$ = 50%), when compared to other collocated instruments such as the particle into liquid sampler (PILS) described previously in chapter 2 (section 2.4.2). *Allan et al.*, [*2004a*] found that if the sampled aerosol flow into the inlet of the instrument is maintained at a high relative humidity, the mass of all the accumulation mode species increases by approximately a factor of 2. They argued that this reduction in $CE_{sulphate}$ was due to the efflorescence of ammonium sulphate particles at lower RH causing the particles to become non-spherical, dropping the $CE_{sulphate}$ to approximately 50%. *CE* should therefore be a function of particle composition and the relative humidity within the inlet, which is dependent on the ambient water vapour concentration and temperature, and the temperature of the laboratory. This indeed was the case for the Edinburgh, Manchester and Jeju Island datasets, where external comparisons with other collocated instruments (e.g. MOUDI or Berner impactors) showed that the AMS particle mass for sulphate was underestimated by a factor of 2 [*Allan et al., 2003a; Topping et al., 2004*].

Clearly different AMS instruments operating in different laboratories at different temperatures may have different values of *CE*. This was the case in PACIFIC 2001, the temperature control in the Slocan Park cabin was poor and often the sampling inlet temperature was higher than ambient (RH low), while the cabin at Langley was well air conditioned (Tsample < Tambient; RH high). The high RH sampling of ammonium sulphate dominated aerosol at Langley taken together with the observations of *Allan et al.*, [*2004a*] leads to the use of a $CE_{sulphate}$ of 100% at Langley and 50% at Slocan. The AMS results were compared to other independent methods of $PM_{2.5}$ measurement (MOUDI and TEOM) [*K. Anlauf and J. Brook, personal communications, Environment Canada, Toronto, Canada, 2003*] at both sites and produced excellent correlations. However, the TEOM and MOUDI reported higher absolute mass concentrations relative to the AMS, particularly at Slocan Park. The comparisons between the AMS and MOUDI mass size distributions for $PM_{1.0}$ indicate that the discrepancy in total mass between the AMS and the other instruments is likely due to the difference in size cuts

between the $PM_{1.0}$ AMS and the other $PM_{2.5}$ instruments. A similar comparison (using MOUDI) was performed at the Sumas site and showed that a $CE_{sulphate}$ of 50% is applicable. On the other hand a comparison of the sulphate mass measured by the AMS and filter samplers at the Jungfraujoch site during CLACE2 experiment revealed that the $CE_{sulphate}$ is only 25%.

AMS results [*Allan et al., 2003a; Alfarra et al., 2004; Boudries et al., 2004*] (and results presented in this chapter) provide indirect evidence that the organic and inorganic components in the accumulation mode are internally mixed based on the similar temporal variability and shape of their modes. It is therefore reasonable to assume a CE of 50% for accumulation mode nitrate, ammonium and organics. To date, there are no studies to determine the CE of the organic material in the small organic mode. Since these organic particles are known to have irregular shapes [*McMurry et al., 1996; Weingartner et al., 1997*], it is probable that they will not be totally focused through the aerodynamic lens and as a result may have a CE less than 100%. A CE of 50% for the small organic particles is assumed in this study. Current experiments to analyse the particle beam shape are underway to investigate the validity of this assumption for future experiments. The CE_s and RIE_s (the latter is discussed in chapter 3, section 3.3) factors used in this thesis are shown in Table 5.1 for each species and location. The RIE_s values in the table have been determined from laboratory calibrations with particles of each species [*Hogrefe et al., 2004*].

Recently, a beam width probe (0.4 mm) has been introduced to many AMS instruments (including the UMIST AMS) to provide more information on the possible divergence of the aerosol particle beam. Results show a well-focused beam when sampling is performed at RH close to saturation or if the shape of the sampled particles is known to be spherical (this was the case during the AMS chamber study discussed in chapter 6), while wider particle beams (i.e. lower CE) are observed at dry conditions. Particle bounce off the vaporiser is likely to explain the observed low CE. Work is still underway to further understand and quantify this behaviour. For example, in the most recent experiments (not discussed in this thesis) the beam width probe has been included and the RH of the inlet system is switched between close to saturation and dry.

Experiment	Collection Efficiency				Relative Ionisation Efficiency			
	CE_{SO4}	CE_{NO3}	CE_{NH4}	CE_{Org}	RIE_{SO4}	RIE_{NO3}	RIE_{NH4}	RIE_{Org}
Edinburgh	0.5	0.5	0.5	0.5	1.2	1.1	4	1.4
Man., winter	0.5	0.5	0.5	0.5	1.2	1.1	4	1.4
Man., summer	0.5	0.5	0.5	0.5	1.2	1.1	4	1.4
Vancouver	0.5	0.5	0.5	0.5	1.15	1.1	3.5	1.4
Langley	1	1	1	1	1.15	1.1	3.5	1.4
Sumas	0.5	0.5	0.5	0.5	1.15	1.1	3.5	1.4
Jeju Island	0.5	0.5	0.5	0.5	1.2	1.1	4	1.4
Jungfraujoch	0.25	0.25	0.25	0.25	1.15	1.1	3.5	1.4

Table 5.1: The collection efficiencies and the relative ionisation efficiencies with respect to the value of IE_{NO3} obtained by using only the ion fragments 30 (NO^+) and 46 (NO_2^+) for each species at all of the sampling locations described in section 5.2. Note that the RIE_{NO3} accounts for the difference between the measured and true IE of ammonium nitrate.

5.3 Overview of chemical composition and size distributions of ambient aerosols

Mass size distributions of the sulphate, nitrate, ammonium and organic fractions of the aerosol particles averaged over the whole sampling period at each of the locations described above are shown in Figure 5.1. It is important to note that these averages are for long periods and they do not show the temporal variability of the particle size distribution, chemical composition and mass concentration. They do, however, provide an overview of the behaviour of the particles at each location over the specified measurement period. A significant accumulation mode with vacuum aerodynamic diameters around 300 – 800 nm, and peaking around 400 – 500 nm was observed at all sites and was principally composed of sulphate, nitrate, ammonium and organic material. Though not shown in panels C in Figure 5.1, the ammonium distribution is similar to that of both sulphate and nitrate. A significant mass mode at a vacuum aerodynamic diameter of about 100 – 200 nm was constantly observed at all urban sites and when fresh or urban air masses affected the other sites [*Boudries et al., 2004*]. This mode was principally composed of organic material with very small concentrations of inorganic species. This finding is consistent with previous observations made in other urban sites in the US [*Jimenez et al., 2003b; Drewnick et al., 2004a*]. The smaller organic mode appears to be characteristic of urban sites and fresh emissions. At non-urban sites, the measurements were often made away from local sources and the small mode became less significant and the distribution was dominated by the accumulation

mode. The disappearance of the small organic mode as the air masses are advected away from urban areas is most likely due to a combination of the effect of coagulation, condensation (which would result in particle growth) and dry deposition.
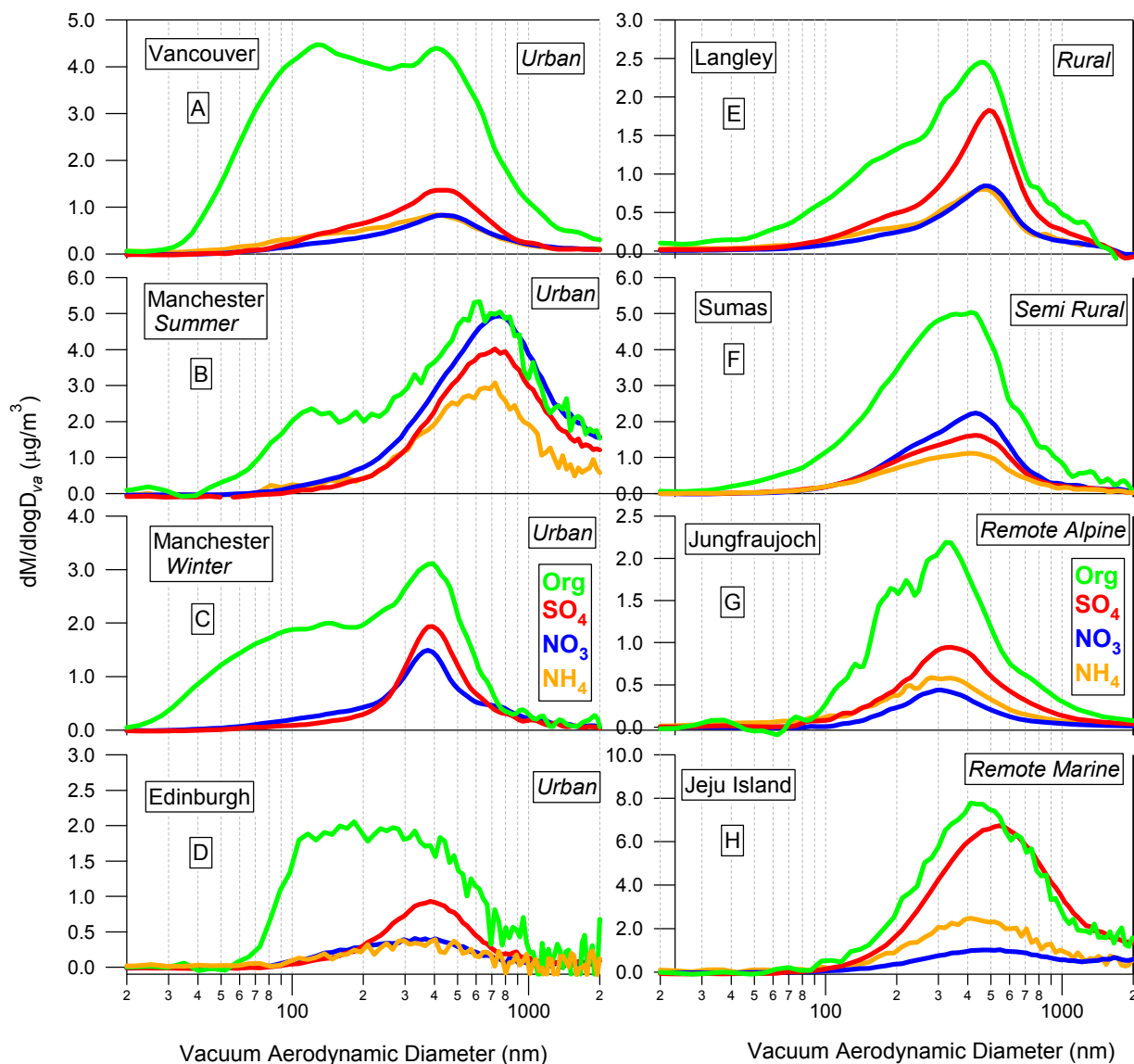

Figure 5.1: Mass size distributions of the organic, sulphate, nitrate and ammonium fractions of the aerosol particles measured by the AMS at various urban, rural and remote locations. Data are averaged over the entire sampling period at each of the locations as described in the text. Note that the different values of the y axis.

A comparison of the observed mass size distributions at all urban sites (panels A – D, Figure 5.1) reveals that they all show consistently similar bimodal organic and monomodal inorganic distributions. However, the average mass size distribution observed in Manchester during the summer sampling period appears to have a significantly larger accumulation mode compared to the other urban sites. This is likely

to be caused by condensation of volatile material on existing particles. The observed difference in the lower size cut off of the measured organic distributions is more likely due to the difference in the particle transmission efficiency of the aerodynamic lens that was upgraded before the Pacific 2001 experiment [*Allan, 2004*]. The temporal variations of the size distributions of the accumulation mode components suggest that they are internally mixed and are indicative of a regional background mode [*Allan et al., 2003a; Boudries et al., 2004*]. Figure 5.2 shows time series mass size distributions ($dM/dlog (D_{va})$) of the sulphate, nitrate and organic aerosol components measured every 15 min in Manchester during the winter sampling period. The data show that all three species have a consistent and temporally similar accumulation mode, with a peak at about 400 nm. The highly time-resolved data in Figure 5.2, also confirms the presence of the consistent smaller organic mode discussed in Figure 5.1. Although they predominantly appear in the accumulation mode, sulphate and nitrate are occasionally measured at smaller sizes [*Allan et al., 2003a*]. The temporal behaviours of the size distributions of sulphate, nitrate and organics at the other sampling locations are similar to those observed in Figure 5.2. The temporal variation in the ammonium size distribution (not shown in the Figure) tends to be similar to that of sulphate and nitrate.

Figure 5.3 presents the average contributions of major chemical components to the total non-refractory mass of submicron aerosol particles at all of the sampling sites described in section 5.2. The total non-refractory mass has been calculated by summing up the mass concentrations of sulphate, nitrate, ammonium and organics. The mass concentration of particulate water has not been included in these calculations. The sulphate contribution to total measured mass ranged from 12% at Slocan Park in Vancouver to 36% at Gosan in Jeju Island. The relatively high abundance of sulphate in the latter location may be attributed to the expected high levels of sulphate precursors such as the naturally emitted dimethyl sulphide (DMS), and sulphur dioxide resulting from coal burning [*Topping et al., 2004*]. Nitrate accounted for 7 – 26% of the total measured mass, while ammonium composed 10 – 16% of the total mass.. The relatively small differences in the contributions of the inorganic components to total mass (with the exception of sulphate in Jeju island), regardless of the sampling location, may

indicate that these fractions of ambient particles are transported regionally, rather than being locally emitted.
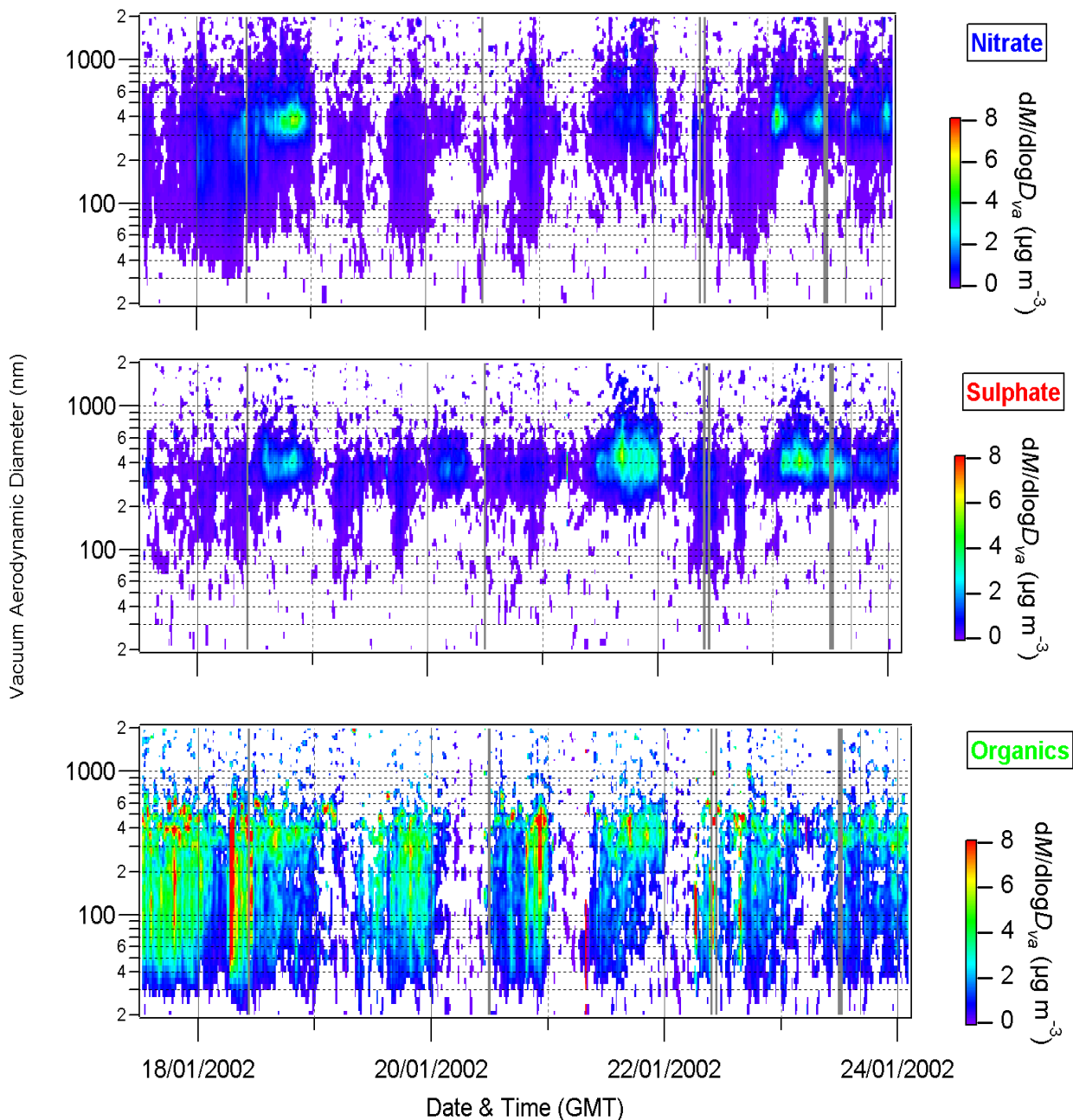

Figure 5.2: Time series of the mass size distributions of the nitrate, sulphate and organic aerosol components measured every 15 min in Manchester during the winter sampling period (see text).
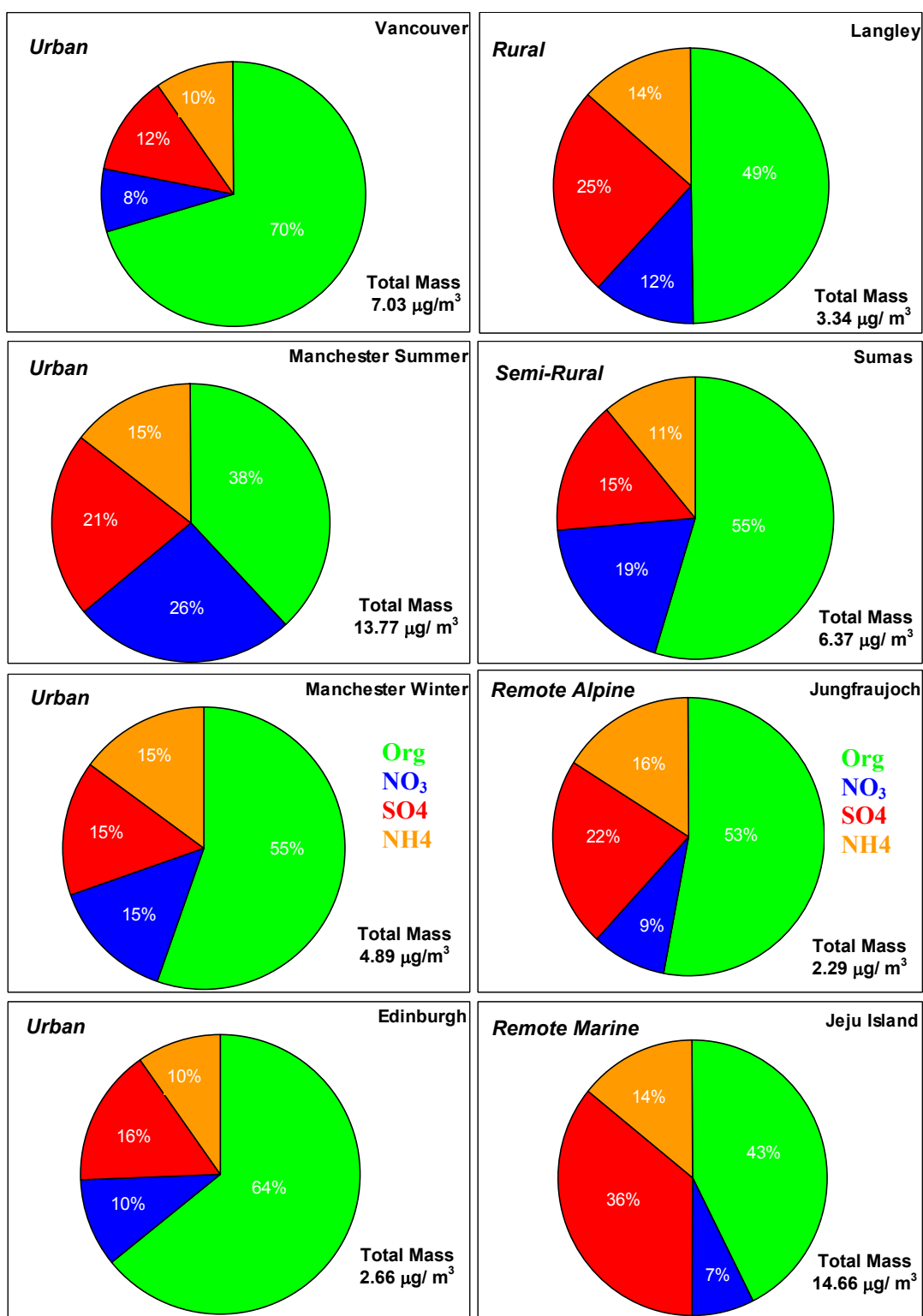
Figure 5.3: Average contributions of major chemical components to the total non-refractory mass of submicron aerosol particles at all of the sampling sites described in section 5.2

On the other hand, results reveal that the organic fraction is the most significant contributor to the total mass measured by the AMS at all of the sampling locations, accounting for 38 − 70% of the total mass. Organic material has been found to account for 70% of the total mass measured at the Slocan Park urban site in Vancouver, which represent an emissions-dominated regime. However, organics accounted for 53% of the total mass measured at the Jungfraujoch high alpine research station, which is a remote site away from local sources. These results illustrate the significance of the organic fraction of ambient aerosols and the need for a better characterisation of its sources, composition and processing.

5.4 Urban organic aerosols

As discussed in section 5.3, the organic fraction of ambient particulate shows a consistent bimodal size distribution at all urban sites, where AMS measurements have been made. The accumulation mass mode peaks at around 450 nm, while the peak of the smaller mode occurs at approximately 150 nm. The sources and chemical composition of those two modes are discussed in detail next.

5.4.1 Sources of urban organic aerosols

In order to determine the sources of the two modes observed in the organic mass size distributions at the Slocan park site in Vancouver (as an example for urban locations), the data was separated by fitting two log normal distributions using a Levenberg-Marquardt non-linear least squares fit [*Press, 1992*]. The area under each fitted mode represents its total organic mass loading. The small organic mode mass loading was significant at the Slocan park urban site almost all of the time, while it was observed only during some periods at the rural site of Langley; suggesting that this mode originated from urban or fresh sources [*Boudries et al., 2004*]. The small organic mass mode was clearly enhanced during periods of high gas phase concentration of CO and volatile organic compounds such as benzene, toluene and 1,3-butadiene. Figure 5.4 shows a correlation between the CO gas phase concentration with the mass concentrations of the fitted small organic mode at Slocan Park in Vancouver [*Alfarra et al., 2004*]. The correlation was quantified using Pearson's *r* values and showed that the small organic mode correlated well with gas phase CO with Pearson's *r* value of 0.76. On the other hand, the same analysis for the large organic mode showed a relatively

weak correlation with gas phase CO with a Pearson's *r* value of 0.58. The results also showed that CO has a background gas phase concentration of 123 ppbv at a limit of zero concentration of small organic particulate at this location. Similar correlations were also calculated for benzene, 1,3-butadiene and toluene and resulted in Pearson's *r* values of 0.79, 0.71 and 0.69, respectively. These gas phase compounds, as well as gas phase CO, are good markers of transport-related emissions and were themselves well correlated within this experiment, with a Pearson's *r* value of 0.75 for CO and 1,3-butadiene. The major source of these trace gases in urban environments is from motor vehicle exhaust. Light-duty vehicles were reported to contribute 63% of the total CO emissions in the Lower Fraser Valley Airshed during the year 2000 [*GVRD, 2002*]. The strong correlation, in Figure 5.4, suggests that combustion-related emissions (with traffic likely representing a large fraction) are the main source of the small organic mode at Slocan Park urban site. The weak correlation between gas phase CO and the large organic mode indicate that other sources contribute to the latter.
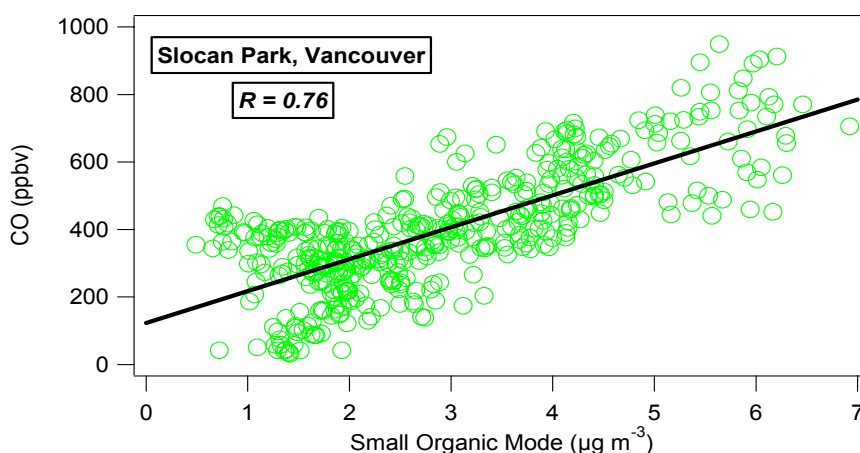

Figure 5.4: A correlation between the concentrations of gas phase CO and the small organic mode during the entire sampling period at Slocan Park, Vancouver. The solid line represents the best data fit.

These findings are consistent with other AMS results, which have been reported for both Manchester and Edinburgh in the UK [*Allan et al., 2003a*]. Figure 5.5 illustrates the strong similarity in the temporal variability in the NO_x gas phase concentration and the integrated mass concentration of organic particulate smaller than 200 nm during the Manchester winter sampling period in January 2001. The U.K. Air Quality Statistics Database and National Atmospheric Emissions Inventory (NAEI) reported that during

1999, transport accounted for 44% and 73% of the NO_x emissions in the UK and Manchester, respectively.
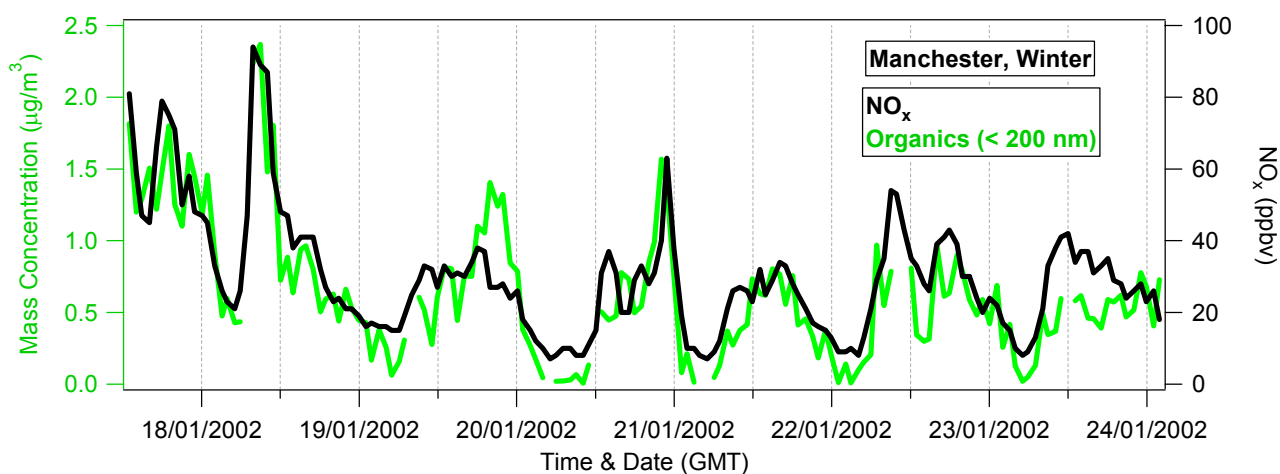

Figure 5.5: Temporal variability of the NO_x gas phase concentrations and the integrated mass concentrations of organic particulate smaller than 200 nm during the Manchester winter sampling period.

The agreement between NO_x and small organic particles has been quantified in Figure 5.6 and covariance between the two resulted in a strong positive Pearson's *r* value of 0.86, suggesting that traffic-related emissions are the main source of the small organic particles observed in Manchester during the sampling period. The small organic mode has also been found to show a similar temporal variation to the traffic flow in Edinburgh during periods where the sampling site was subjected to air masses from the city direction. These results are similar to those found in Vancouver and demonstrate that traffic could be the main source of the observed small organic mode at urban sites.
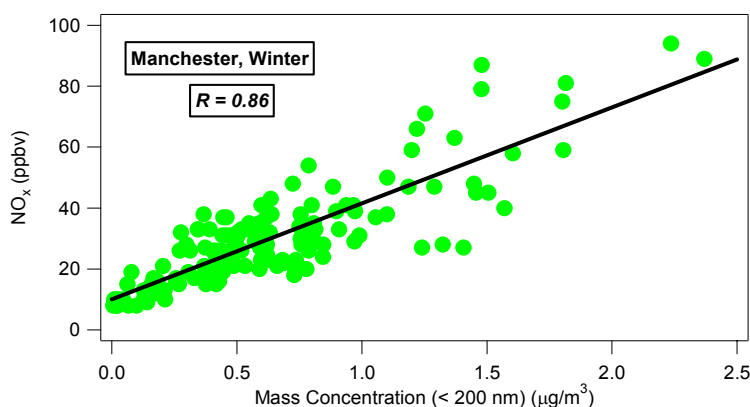

Figure 5.6: A correlation between the concentration of gas phase NO_x and the integrated mass concentration of organic particulate smaller than 200 nm during the Manchester winter sampling period. The solid line represents the best data fit.

5.4.2 Chemical composition of urban organic particulate

The laboratory results discussed in chapter 4 (section 4.2) have shown that mass spectra obtained using the AMS compare well to the NIST standard library of mass spectra for a range of chemical compounds with the exception of highly oxidised organic compounds such as oxo-, di- and poly-carboxylic acids and humic-like substances (see section 5.6.3), where m/z 44 (CO_2^+) was found to be much more pronounced in the AMS spectra. The enhanced m/z 44 signal was coupled with a very strong peak at m/z 18 indicative of H_2O^+, implying thermal breakdown of the carboxylic acid group on the vaporiser. This phenomenon is reproducible and, coupled with the fact that m/z 44 is generally small when sampling primary aerosol materials such as hydrocarbons, allows us to use this peak as an indicator of highly oxidised organic compounds measured by the AMS. It is important however to note that m/z 18 also receives large contributions from gas phase water, sulphate and other species. To retrieve the total organic mass loading, the contribution of water resulting from decarboxylation at m/z 18 is set equal to m/z 44 based on laboratory results with pure compounds performed in Argon, where the interferences to m/z 18 are eliminated [*P. Silva, Utah State University, Personal Communication*]. As a result, there is no independent information about the mass spectral signature of the observed organic in these experiments at m/z 18.

The m/z 43 is a characteristic fragment of both saturated hydrocarbon compounds ($C_3H_7^+$) and oxidised organic compounds such as aldehydes and ketones (CH_2CHO^+ or CH_3CO^+). On the other hand m/z 57 is a typical fragment of saturated hydrocarbon compounds ($C_4H_9^+$) and receives a negligible contribution from oxidised organic compounds. A correlation of the mass concentration of m/z 57 with the concentration of the established primary gas phase marker CO at the urban site in Vancouver had a Pearson's r value of 0.74, while a similar correlation using m/z 44 at the same location had a Pearson's r value of 0.42. Similar correlations have been performed with the Manchester winter data using NO_x as a primary marker and resulted in Pearson's r values of 0.85 and 0.24 for m/z 57 and m/z 44, respectively. These correlations support the selection of m/z 57 as a primary marker in the AMS data and may role out any significant contribution of primary emissions to m/z 44.

Figure 5.7 shows the mass size distributions of the three key organic mass fragments discussed above averaged over the whole sampling period at each of the urban sampling location described in section 5.2. The *m/z* 44 shows a pronounced mostly monomodal distribution, with a modal diameter of about 400 - 450 nm in the Vancouver and Manchester winter data. A similar monomodal distribution with a larger modal diameter of about 700 nm has been observed for *m/z* 44 in the Manchester summer data. This is a strong evidence of internal mixing between oxidised organics and sulphate in the Manchester summer data, as the latter shows a similar increase in the modal diameter at this location as discussed in section 5.3. The distribution for *m/z* 44 is not available for the Edinburgh data, because this mass fragment was not scanned in the TOF mode of
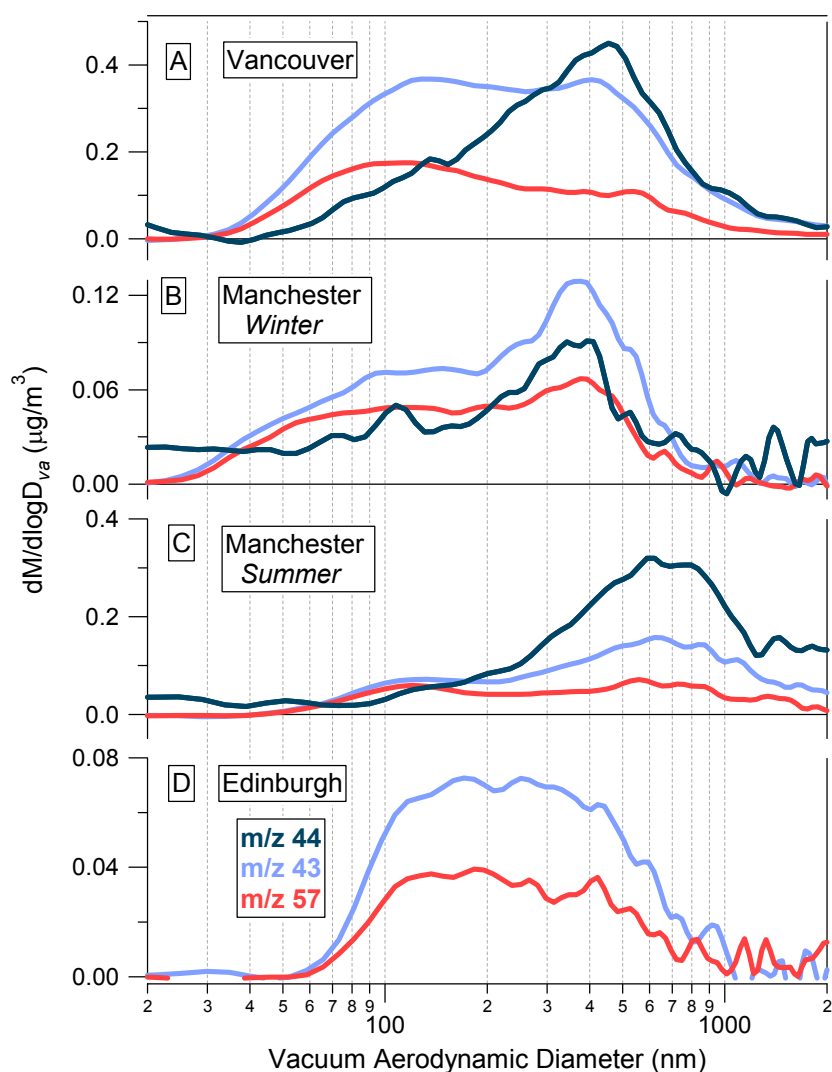

Figure 5.7: Mass size distributions of selected organic mass fragments averaged over the sampling duration at the urban locations described in section 5.2.

operation during this experiment. The domination of a monomodal distribution of *m/z* 44 in the urban sites implies that there is little contribution from highly oxidised organic compounds in the small organic mode. In addition, the relative magnitudes of *m/z* 44 to the other two fragments indicate the presence of more oxidised organic compounds in the Manchester summer and Vancouver data relative to that of Manchester winter.

The other two mass fragments (*m/z* 43 and 57) show bimodal mass size distributions similar to that observed for the total organic aerosol fraction shown in Figure 5.1. The relative magnitudes of the small and large modes for *m/z* 43 and *m/z* 57 reflects the contribution of different sources to these mass fragments, in particular the contribution of oxidised organics to *m/z* 43 as discussed above. For example, in the Manchester summer data the two modes of *m/z* 57 have similar peak magnitudes, while the accumulation mode is larger than the small mode in the case of *m/z* 43 indicating that oxidised species contribute more to *m/z* 43 than *m/z* 57 in the accumulation mode size range.

More information on the chemical composition of urban organic aerosols can be derived from their mass spectral signatures. Panel C in Figure 5.8 shows a mass spectrum of diesel bus exhaust aerosol obtained by *Canagaratna et al.*, [*2004*] in a recent "vehicle chasing" study using an AMS instrument identical to the one described here. The study was designed to characterise both gaseous and particulate matter emissions from individual in-use vehicles under real world driving conditions in New York City. The diesel exhaust spectrum was compared to laboratory generated diesel fuel (panel A) and lubricating oil (panel B) spectra and the study concluded that under most operating conditions the organic carbon fraction of in-use diesel vehicle exhaust aerosol is dominated by the recondensed vapor from the evaporated engine lubricating oil. These findings were similar to those found by *Tobias et al.*, [*2001*] and *Sakurai et al.*, [*2003*], which also concluded that the dominant organic components of fuel and lubricating oil are n-alkanes, branched alkanes, cycloalkanes, and aromatics (including polyaromatic hydrocarbons). All spectra were dominated by the ion series $C_nH_{2n+1}^+$ (*m/z* 29, 43, 57, 71, 85…), which is typical of saturated normal and branched alkanes. Other important ion series were also observed including $C_nH_{2n-1}^+$ (*m/z* 27, 41, 55, 69,83…) typical of

alkenes, $C_nH_{2n-3}^+$ (*m/z* 67, 79, 81, 95, 107, 109…) typical of cycloalkanes and $C_6H_5C_nH_{2n}^+$ (*m/z* 77, 91, 105, 119…) typical of aromatics [*McLafferty and Turecek, 1993*][*McLafferty and Turecek, 1993*].
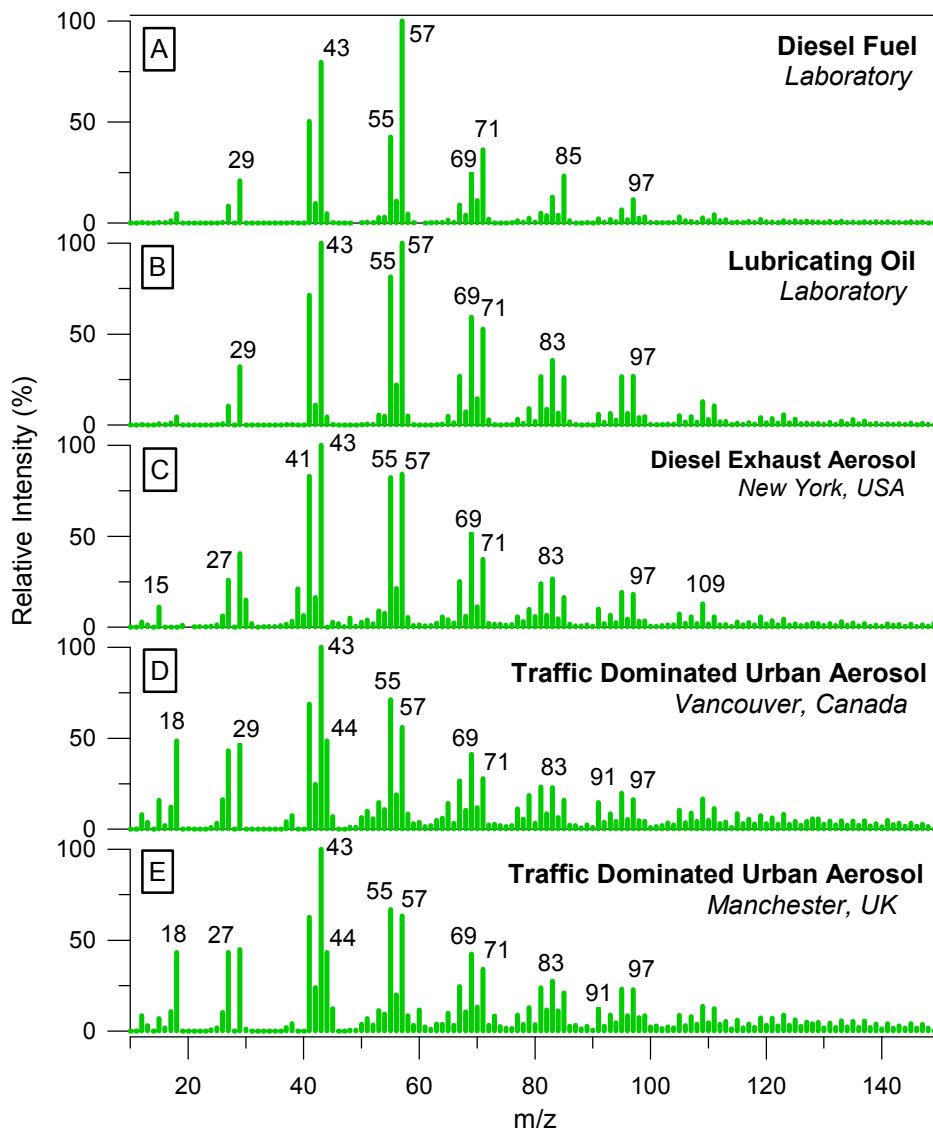

Figure 5.8: Mass spectra of the organic aerosol component measured from diesel fuel and lubricating oil laboratory samples and at various urban locations.

Panel D in Figure 5.8 shows a mass spectrum of the organic fraction of the ambient particles measured at the Slocan Park urban site in Vancouver during periods dominated by traffic emissions. A similar mass spectrum is shown in panel E for the Manchester winter sampling period. The spectra are averages of the organic particulate composition during all periods where CO concentrations were higher than the local averages (403 ppbv in Vancouver and 289 ppbv in Manchester winter). A comparison of the ambient

organic mass spectra in panels D and E with that in panel C suggests a significant similarity in the chemical composition of the traffic-dominated ambient organic particulate in Manchester and Vancouver and that of diesel exhaust organic particulate in New York City. The similarity of the ambient spectra and the laboratory generated lubricating oil spectrum indicates that recondensed vapour from engine lubricating oil dominated the organic fraction of ambient particulate in Manchester and Vancouver during the sampling periods. A closer inspection of the spectra in Figure 5.8 shows that the ambient spectra have an extra fragment at *m/z* 44, a more enhanced *m/z* 43 relative to its adjacent fragments and a more abundant *m/z* 55 relative to *m/z* 57. Oxidised organic compounds contributing to the separate accumulation mode are likely to be the sources of these subtle differences.

5.5 Rural and remote organic aerosols

As discussed in section 5.3, the averaged size distributions of the organic fraction at locations away from particle source points are clearly different from these observed at urban sites (see Figure 5.1). The organic distributions in the former case are dominated by an accumulation mode with a peak around 300 - 450 nm, with variable smaller, broad mode below 200 nm. This is consistent with the sampling sites having fewer sources of fresh emissions as compared to urban areas. Figure 5.9 shows mass size distributions of the three key organic mass fragments discussed in section 5.4.2, averaged across the sampling durations at each of the non urban sites described in section 5.2.

The dominance of mass fragments 44 and 43 in the accumulation mode and the lack of significant contributions from mass fragments 57 and 43 in the small mode (compared to their observed distributions at the urban sites shown in Figure 5.7) suggest that organic particulate at these sites has a large contribution from oxidised compounds, and that secondary organic aerosols are more significant than primary organic aerosols at these locations during the sampling periods. Each of the mass fragments seems to have similar size distributions at all of the four locations. However the *m/z* 44 appears to be more pronounced relative to *m/z* 43 at the Jungfraujoch and Jeju Island remote sites,

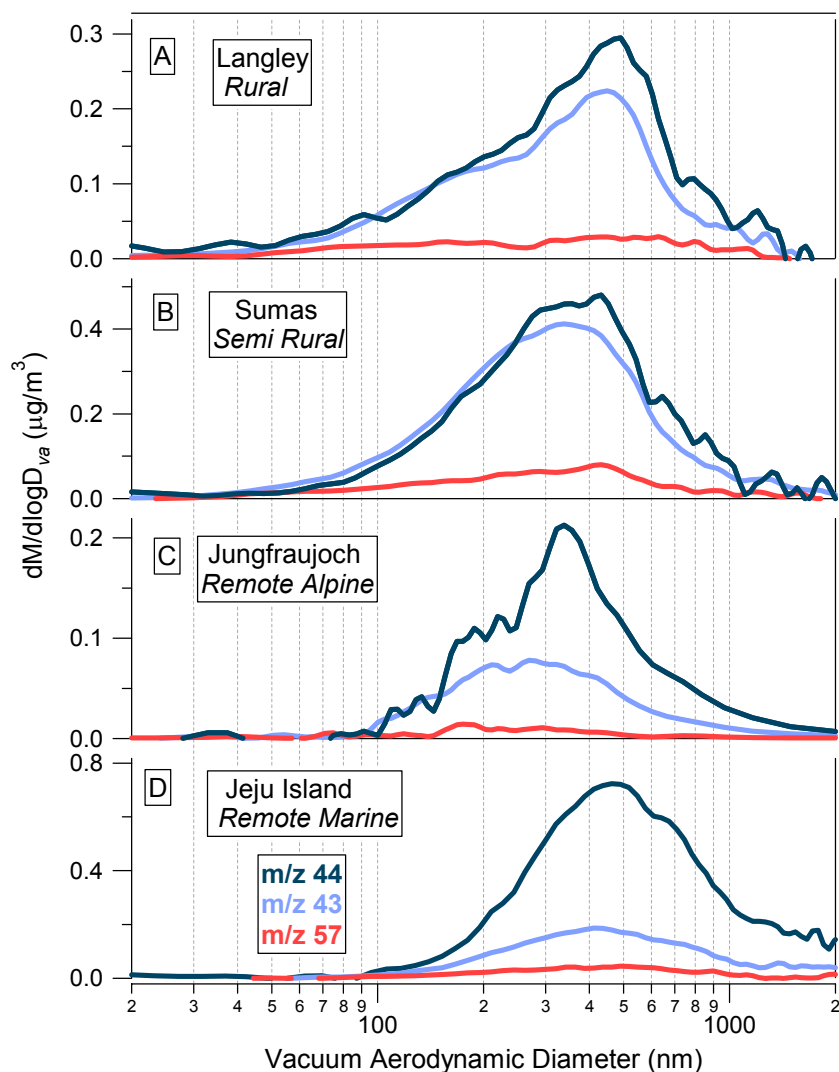suggesting more atmospheric processing at those locations relative to Langley and Sumas sites.

Figure 5.9: Mass size distributions of selected organic mass fragments averaged over the sampling duration at the non-urban locations described in section 5.2.

This is further confirmed in Figure 5.10, which shows mass spectra of the organic aerosol fraction averaged over the sampling duration at each of non-urban sites. The mass spectral signatures are similar at all sites and the most significant contributions to these spectra arise from mass fragments characteristic of oxidised organic compounds such as *m/z* 44 in addition to mass fragments 43 and 55. The rural and semi rural spectra (panels A and B, receptively) show some contribution from fragments typical of aromatic and cyclic compounds such as 67, 79, 91, 95 and 105. However, the spectra in

panels C and D show that these mass fragments are much less observed at the Jungfraujoch and Jeju Island remote sites, supporting the argument that organic particulates have been exposed to more processing at those two locations. This argument will be discussed in more detail in the next section of this chapter.
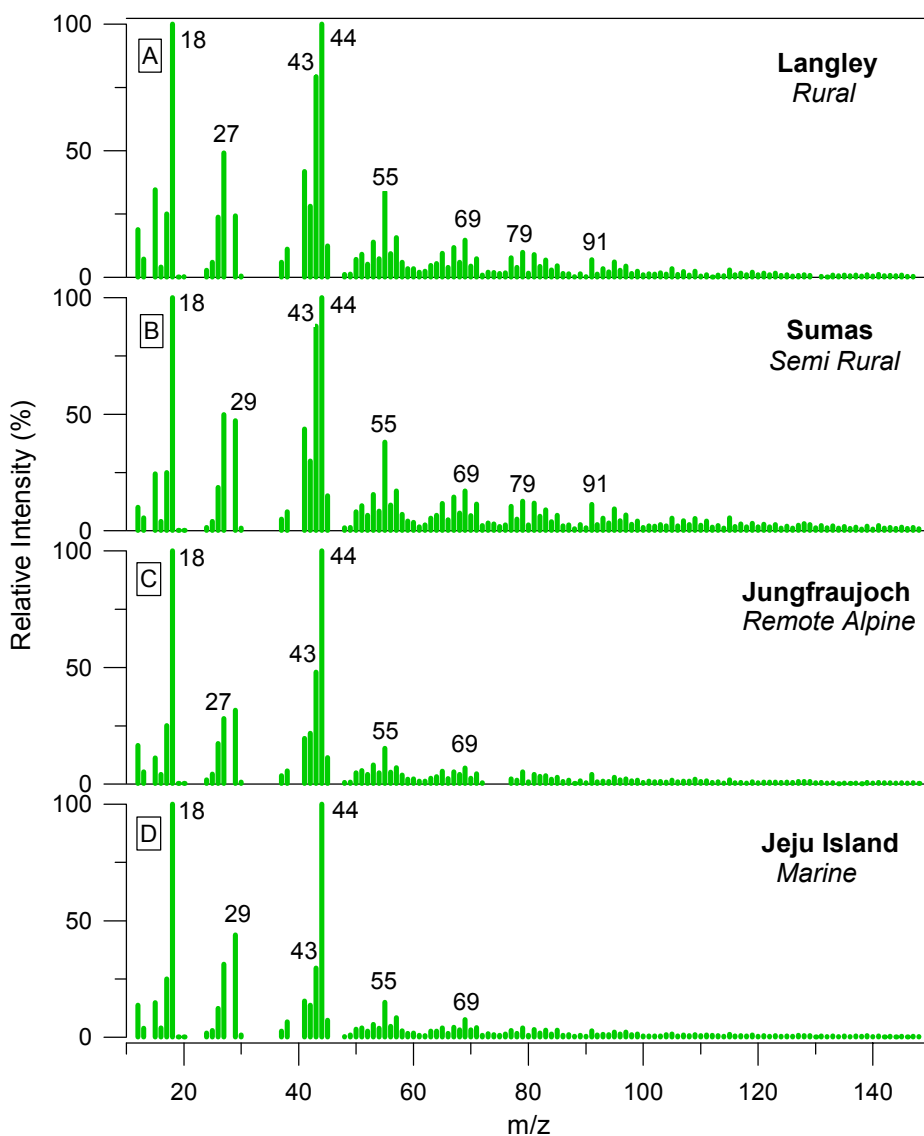

Figure 5.10: Mass spectra of the organic aerosol component measured at the non-urban locations described in section 5.2.

The relationship between the organic aerosol and gas phase marker compounds at the Langley site was investigated in order to further understand the possible sources of the organic particulate at this location. Similar to the analysis applied to the Slocan Park data in section 5.4.1, two log normal distributions were fitted to the Langley data in an

attempt to understand the behaviour of the two organic modes at this rural location. However, as the two modes were typically less distinct than at the Slocan Park urban site, the fits converged less often and the fitted parameters had to be treated carefully. Any fitted distributions that did not result in a turning point between the two peaks were treated as mono modal. The total mass loading of each mode was compared with the concentration of the gas phase species CO, NO, SO_2, O_3, peroxyacetyl nitrate (PAN), and NO_y; the total sum of oxidised nitrogen-containing compounds. The correlations were quantified using Pearson's r values as illustrated in Figure 5.11, and were calculated for the whole AMS sampling period at Langley from August 11 to September 01 2001. Gas phase data were available for most species at most times except for NO and NO_y, for which there were no data between the 21 and 26 August. In addition there were no CO data available between the 17 and 21 August.
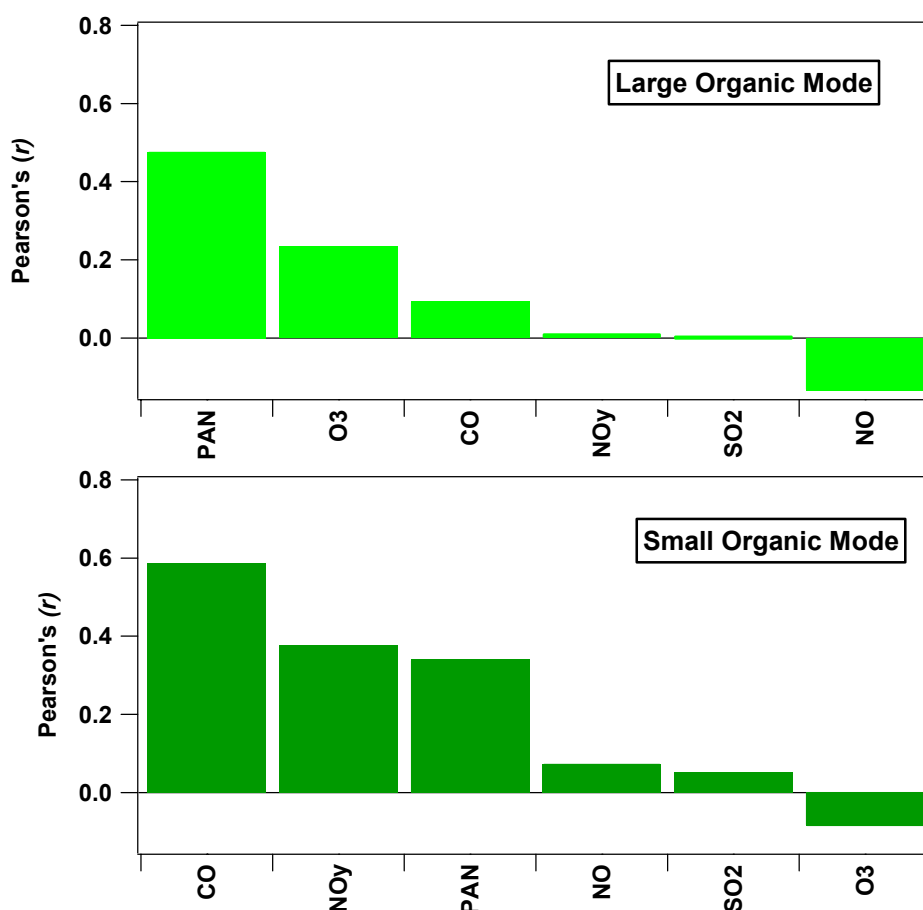

Figure 5.11: Correlations between various gas phase compounds with the large organic mode loading (top panel) and the small organic mode loading (bottom panel) at the Langley site.

The small organic mode had the strongest correlations with CO and NO_y (which includes NO_x) indicating that a significant part of this mode originated from combustion sources; similar to that found at the Slocan Park site. On the other hand, the large accumulation organic mode had the strongest correlations with PAN and O_3, which are indicators of photochemical oxidation and production, respectively. The correlations in Figure 5.11 combined with the size distributions in panel A of Figure 5.9 suggest that the small organic mode was mainly observed when the Langley site was exposed to recent combustion emissions, while a large fraction of the accumulation mode was a result of secondary aerosol formation and/or aerosol photochemical processing. These findings are in agreement with observations, which have been reported by a number of researchers regarding the importance of polar organics in particles in rural and remote regions. For example, infrared spectroscopy was used to illustrate the predominance of polar organics in submicron particles in a relatively remote site in the Smoky Mountains, Tennessee, USA [*Blando et al., 1998*]. In a study of long range transport of air pollution in central Japan, dicarboxylic acids were shown to comprise as much as 30 – 50% of the total organic particulate matter and most of them were estimated to be formed by oxidation of precursors in air [*Satsumabayashi et al., 1989; Satsumabayashi et al., 1990*]. The chemical composition of organic particulate in rural and remote regions is discussed in more detail in section 5.6.3.

5.6 Processing of organic aerosols

5.6.1 Comparison of 'fresh' and 'processed' organic aerosols

The graphs in Figure 5.12 classify organic particulate measured at urban locations in Manchester (Panel A), Vancouver (Panel B) and at a rural location in Langley, Canada (Panel C) as a function of the CO and O_3 concentrations observed at these locations during the same measurement periods. Each panel (A-C) shows two organic mass size distributions averaged over conditionally selected periods. The selection criteria for the first distribution in panels (A-C) are that CO concentrations are higher than the local mean value and O_3 concentrations are lower than the local mean value (hereafter referred to as HC & LO). The second distribution in panels (A-C) has the converse criteria of HO & LC applied. Table 5.2 shows the local mean concentrations of CO and O_3 at each site. The HC & LO periods indicate a higher than average influence of

combustion-related emissions and lower than average secondary oxidant availability, while the HO & LC periods discriminate in favour of periods of opposite conditions. The averages over the HC & LO periods should therefore represent periods when the small organic mode is enhanced and the averages over the HO & LC periods should reflect increased secondary aerosol formation. Also shown in panels (A-C) are the organic mass spectral signatures obtained in these contrasting situations. The average mass spectra acquired during the HC & LO periods are shown for the urban experiments in panels A and B and that acquired during the HO & LC periods is shown in panel C.

Location	O_3 (ppbv)	CO (ppbv)
Manchester, UK	12	289
Vancouver, Canada	18	403
Langley, Canada	19	180

Table 5.2: Local mean concentrations of O_3 and CO used in the conditional averaging of organic size distributions in Figure 5.12.

In both Vancouver and Manchester the organic mass loading is considerably higher during the HC & LO periods relative to the HO & LC periods. This is largely a function of turbulent mixing. During stable, poorly mixed conditions, the emissions of CO, particles and NO are elevated, the latter titrating the available O_3. During well-mixed periods dilution significantly reduces the concentration of the emitted species and regional O_3 is entrained into the city. At the rural site, O_3 and other secondary oxidants have had time in the atmosphere to form and are often elevated, whereas the influence of urban sources is intermittent and dependent on the synoptic meteorology at the time. The latter is reflected in the highly variable CO concentrations observed.

The graphs in Figure 5.12 show that organic aerosols had bimodal size distributions during the HC & LO periods at urban locations (A, B), as discussed in section 5.4. During HO & LC periods a more significant accumulation mode relative to the small mode was observed. On the other hand, the organic size distribution at the rural site, panel C, shows a dominant accumulation mode relative to a broad and less defined smaller mode in both conditionally averaged cases. However, a comparison of the

organic distribution during HC & LO periods to that of HO & LC periods shows that the former has a broader small organic mode suggesting more fresh emissions during the HC & LO periods into a background of a large mass of accumulation mode oxidised organic aerosol.

The organic mass spectra averaged during the HC & LO periods at both urban locations seem to have almost the same fragments; indicating that the chemical composition of the recently emitted organic particulate in Manchester and Vancouver is likely to be very similar. Which, when compared with laboratory generated mass spectral signatures (discussed in section 5.4.2), implies a mixture of saturated and un-saturated hydrocarbons, cyclic compounds and some aromatics. The mass spectrum in panel C shows the averaged chemical composition of organic particulate during HO & LC periods at the rural site. The spectrum looks clearly different to those of the fresh urban aerosols in graphs A and B. It is dominated by mass fragments that are typical of oxidised organic compounds such as m/z 44, signatures of di- and poly- carboxylic acids, in addition to mass fragments 43 and 55 which can be associated with other types of oxidised organic compounds including aldehydes and ketones [*McLafferty and Turecek, 1993*]. The hydrocarbon contribution to mass fragments 43 and 55 is likely to be small in this spectrum as the signal at m/z 57 is almost negligible and the small organic mode is negligibly small during the HO & LC periods. The spectrum also contains very small contributions from mass fragments typical of cyclic compounds such as m/z 67 and 79 in addition to aromatic fragments like m/z 91. The presence of relatively high molecular weight fragments in the urban spectra represents another significant difference between the rural and urban organic particulate, suggesting that secondary organic aerosols or the processed primary organic compounds produce shorter carbon chain fragments. The rate of this transformation will be enhanced during periods of enhanced O_3 concentrations when oxidant availability is high.
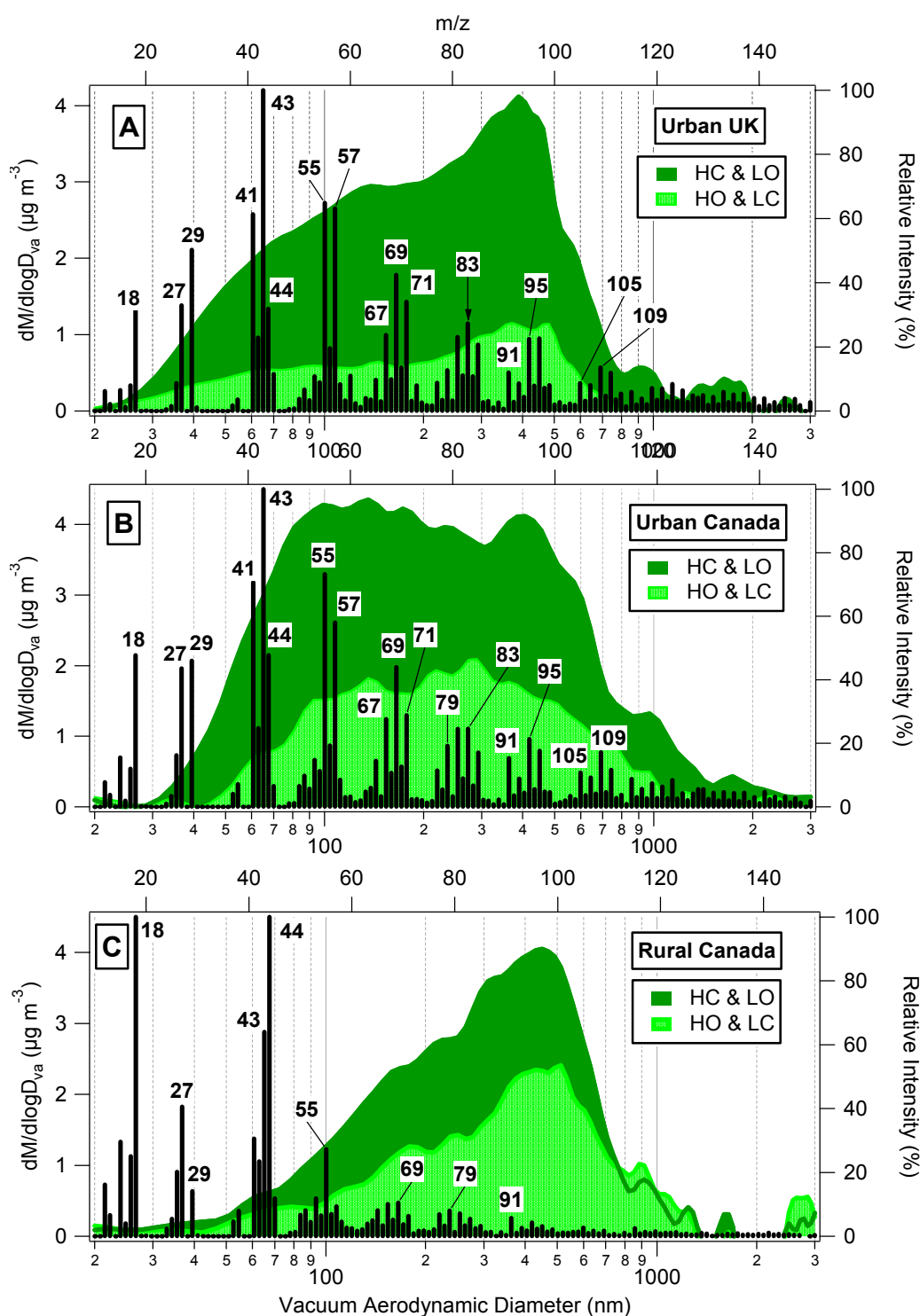
Figure 5.12: Mass size distributions of organic particulate conditionally averaged (see text). The data shown are for urban locations in Manchester, UK (Panel A), Vancouver, Canada (Panel B) and rural Canada (Panel C). The average organic mass spectra acquired during HC & LO (high CO and low O_3 respectively, see text for details) periods are shown for the urban locations (Panels A and B) and that acquired during HO & LC periods is shown for the rural location (Panel C).

5.6.2 Influence of photochemistry on the chemical signature and size distribution of organic aerosols

A bimodal size distribution with a significant combustion-related small organic mode composed of hydrocarbons and aromatics has been found to be typical of urban sites. However, during the first few days of sampling at Slocan Park in Vancouver, the site was exposed to a photochemical episode where the O_3 level reached $\sim$ 80 ppbv at times (compared to a mean level of 18 ppbv during the sampling duration). Figure 5.13 shows an averaged organic mass size distribution and mass spectrum averaged over all periods where O_3 concentrations exceeded 50 ppbv at Slocan Park in Vancouver.
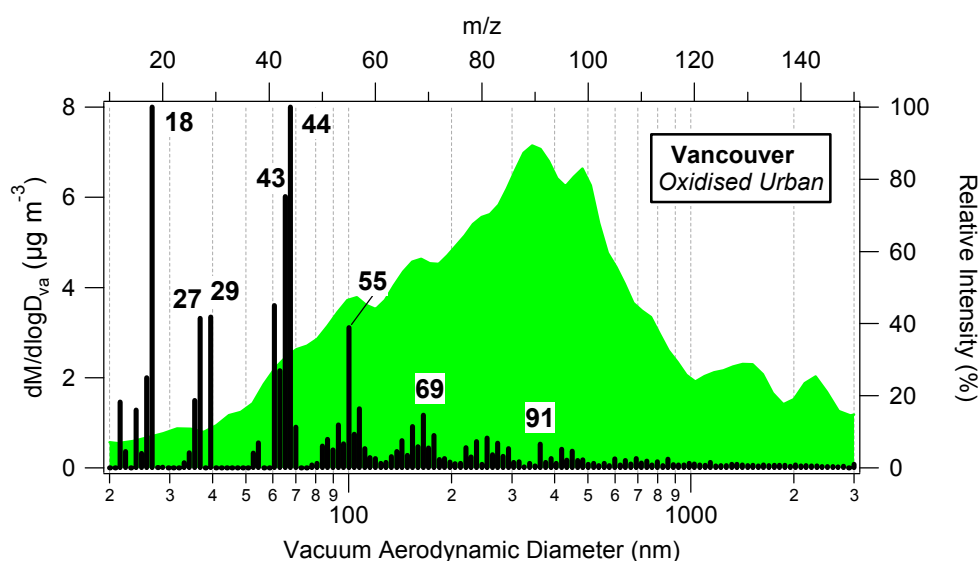

Figure 5.13: A mass size distribution and a mass spectrum of ambient organic aerosols averaged over all periods where O_3 concentrations exceeded 50 ppbv at Slocan Park, Vancouver, during Pacific2001.

In contrast to the average organic size distribution across the whole experiment shown in panel A of Figure 5.1, the organic distribution in Figure 5.13 shows that during this period of intensive photochemistry the typical bimodal organic distribution became less apparent and the accumulation mode was significantly enhanced and dominated the distribution with a mass loading almost twice its average value. The mass spectrum in Figure 5.13 represents the averaged chemical composition of the oxidised urban organic particulate during these same periods. The most significant features of this spectrum are the high abundance of *m/z* 44 in addition to the high ratio of *m/z* 55 relative to 57; both are characteristic of oxidised organic compounds. Other hydrocarbon and aromatic-

related ion series can still be observed, as their combustion-related sources always exist at this urban site. A similar mass spectrum has also been observed in the Manchester summer data, where the averaged accumulation mode was larger in size than Manchester winter, suggesting that photochemical activity was high in Manchester during most of that sampling period.

Similar to Slocan Park in Vancouver, the rural Langley site was also exposed to the relatively high O_3 concentrations in what appeared to be a regional photochemical episode. Figure 5.14 shows organic mass spectrum and size distribution conditionally averaged in a similar way to Slocan Park using O_3 concentration of 50 ppbv (the mean O_3 concentration during the sampling duration was 19 ppbv). Unlike the double selection criteria used in Figure 5.12, a single criterion is used in here due to the lack of CO data during periods of relatively elevated O_3 concentrations. However, the relatively elevated O_3 and CO periods were mutually exclusive at Langley when both datasets were available. Interestingly, the organic aerosol processing during the relatively high O_3 episode seems to have increased the modal diameter of the accumulation mode at Langley from about 400 nm to 600 nm and almost doubled its mass loading. The mass spectrum in Figure 5.14 represents an averaged organic composition during the relatively high O_3 periods at Langley and shows very similar signature to that previously discussed in Figures 5.10 and 5.12 for this rural site.
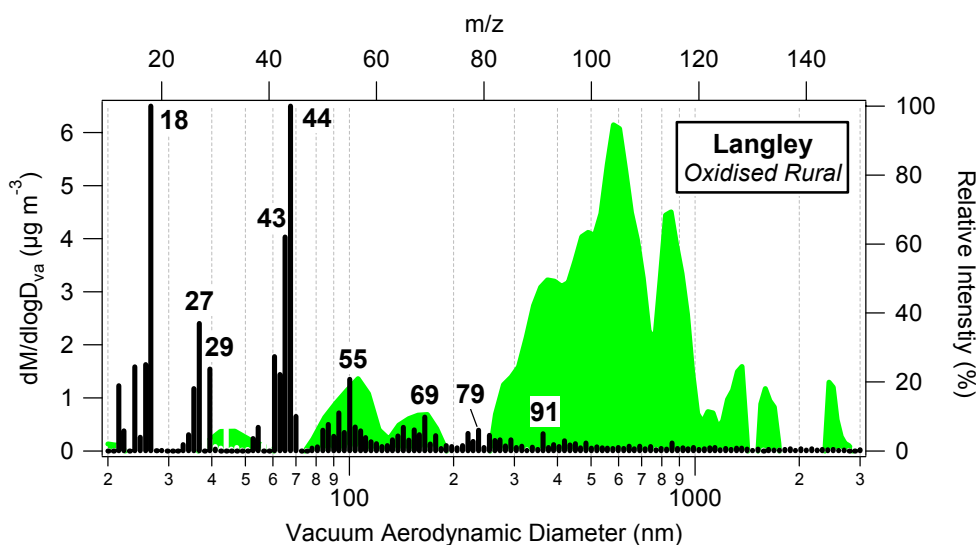

Figure 5.14: A mass size distribution and a mass spectrum of ambient organic aerosols averaged over all periods where O_3 concentrations exceeded 50 ppbv at Langley during Pacific2001.

5.6.3 Chemical composition of processed organic aerosols

To date, only 10 − 15% of the organic mass have been resolved and identified on a molecular level [*Rogge et al., 1993; Puxbaum et al., 2000*]. This has been mostly attributed to the fact that high-molecular weight organic (i.e. > C40) and highly polar compounds cannot be analysed with standard GC/MS methods. In addition, some organic compounds are not easily extracted or their GC/MS signatures cannot be confirmed by standards [*Rogge et al., 1993; Saxena and Hildemann, 1996*]. As a result, more than 80% of the molecular composition of the ambient aerosol organic fraction remains unknown. However, water-soluble macromolecular substances with spectral properties of "humic-like substances" (HULIS) have recently been found to contribute 20 − 50% to the water-soluble fraction of organic aerosol at urban and rural sites in Europe [*Havers et al., 1998; Facchini et al., 1999a; Zappoli et al., 1999; Krivacsy et al., 2000; Krivacsy et al., 2001b*]. HULIS are composed of hundreds of different molecules, which cannot be separated, and therefore cannot be individually identified and quantified [*Krivacsy et al., 2001b*]. *Limbeck et al.*, [*2003*] stated that the primary sources of HULIS identified so far, such as biomass burning, are not adequate to explain the observed HULIS levels in Europe, and showed that secondary aerosol formation of atmospheric polymers occurs by heterogeneous reaction of isoprenoid (e.g. isoprene) or terpenoid (e.g. α-pinene) emissions in the presence of a sulphuric acid aerosol catalyst. In addition, recent smog chamber studies have reported the formation of oligomers and polymers in secondary organic aerosol (SOA) produced from the photooxidation of anthropogenic and biogenic precursors [*Kalberer et al., 2004; Tolocka et al., 2004a*]. The AMS has recently been utilised to study the chemical signatures of these SOA products in a reaction chamber and results are discussed in the next chapter.

The presence and characterisation of HULIS in aerosol samples have been achieved using a number of methods. *Krivacsy et al.,* [*2001*] reported that in alkaline solutions, these compounds are ionic and capillary electrophoresis can be a simple but effective technique to indicate their presence in samples. Infrared spectroscopy (IR) has been widely used for the characterisation of HULIS in atmospheric samples [*Mukai and Ambe, 1986; Havers et al., 1998; Limbeck et al., 2003*], and indicated that carboxylic

groups (COOH), hydroxyl groups (OH) and carbonyl groups (C=O) are the main functional groups of HULIS. Proton nuclear magnetic resonance spectroscopy (HNMR) has been used in combination with ion exchange chromatography and total organic carbon analysis for the speciation and quantification of the WSOC of aerosol and fog samples [*Decesari et al., 2000*]. Results showed that the complex mixture of aerosol/fog WSOC was separated into three main classes of compounds: 1) neutral and/or basic compounds; 2) hydroxy-, mono-, and di-carboxylic acids; 3) polyacidic compounds. Characterisation by HNMR spectroscopy showed that class 1 is mainly composed of polyols or polyethers, class 2 is mainly composed of hydroxylated aliphatic acidic compounds, while class 3 is composed of highly unsaturated polyacidic compounds of predominantly aliphatic character, with a minor content of hydroxyl groups. The study found that model structures, analogous to HULIS, consisting of an aromatic core bearing substituted aliphatic chains (with –COOH, -CH$_2$OH, -COCH$_3$, or -CH$_3$ terminal groups) properly fit the HNMR features observed in the third class. *Decesari et al.,* [*2000*] also reported that a commercially available standard of humic substance (Suwannee River Fulvic acid Reference) exhibits a chromatographic behaviour similar to that of class 3.

As a result of the demonstrated importance of HULIS, an AMS spectrum of a standard fulvic acid reference was obtained using particles generated using the laboratory setup described in section 4.1. Interestingly, the AMS mass spectrum of fulvic acid (panel A, Figure 5.15) is dominated by *m/z* 44. As discussed in section 4.2, this mass fragment arises from CO$_2^+$ and has been identified as the AMS signature of highly oxidised compounds such as hydroxy- and di-carboxylic acids. There is also a significant contribution from *m/z* 18 due to the associated H$_2$O$^+$ in the decarboxylation process. Similar to dicarboxylic acids in section 4.2, the contribution of mass fragment 18 to the fulvic acid mass spectrum has been calculated by subtracting the air beam contribution to *m/z* 18 assuming the particles are dry. This is not possible to retrieve from ambient data due to interferences from sulphate and gas phase and particulate water, and as a result *m/z* 18 is set to equal *m/z* 44 as an estimation of the minimum contribution of *m/z* 18 to the organic mass.

Figure 5.15 compares the fulvic acid mass spectrum signature with ambient organic mass spectra obtained from the urban, rural and remote locations described in this chapter. The comparison reveals that the mass spectral signatures of organic particulate in the remote, rural and oxidised urban sites are highly similar to that of humic-like compounds and were all dominated by *m/z* 44. On the other hand, the traffic dominated organic spectrum measured in Vancouver showed a different signature to that of fulvic acid, where *m/z* 43 and other aliphatic fragments were far more dominant than *m/z* 44.
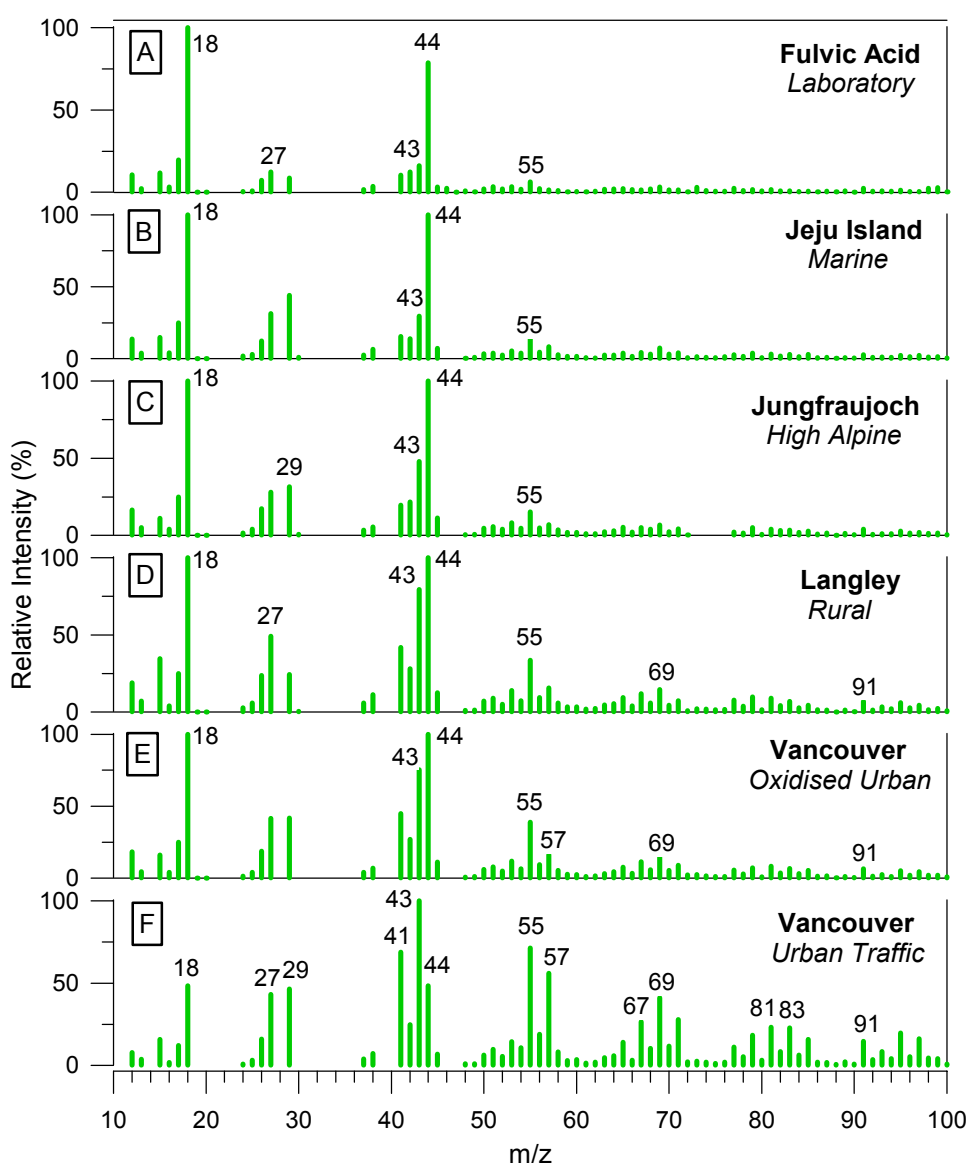

Figure 5.15: Mass spectral signatures of laboratory generated fulvic acid and organic aerosols measured in various urban and non-urban locations

The similarity among the ambient spectra in Figure 5.15 and the fulvic acid spectrum was quantified by scattering the values of each mass spectrum against those of fulvic acid and calculating the Pearson's r values as shown in Figure 5.16 and summarised in Table 5.3. Similar correlations have been also performed between the fulvic acid mass spectrum and ambient organic spectra from traffic dominated periods from the Manchester winter sampling period, diesel exhaust from New York City and laboratory generated lubricating oil and diesel fuel spectra. The Pearson's r values of these correlations are also included in Table 5.3. The change in the organic mass spectral signature from urban to remote sites, in Figure 5.15, and the increasing similarity with the fulvic acid spectra, as quantified in Table 5.3, provide clear evidence that atmospheric processing of ambient aerosols results in highly oxidised organic fraction.

Location	Pearson's r value
Jeju Island, *remote Marine*	0.96
Jungfraujoch, *high alpine*	0.95
Langley, *rural*	0.87
Vancouver, *oxidised urban*	0.87
Vancouver, *traffic urban*	0.50
Manchester, *traffic urban*	0.46
New York, *diesel exhaust*	0.14
Laboratory, *lubricating oil*	0.14
Laboratory, *diesel fuel*	0.15

Table 5.3:Pearson's r values of the correlations between the fulvic acid mass spectrum and organic spectra measured in various locations.
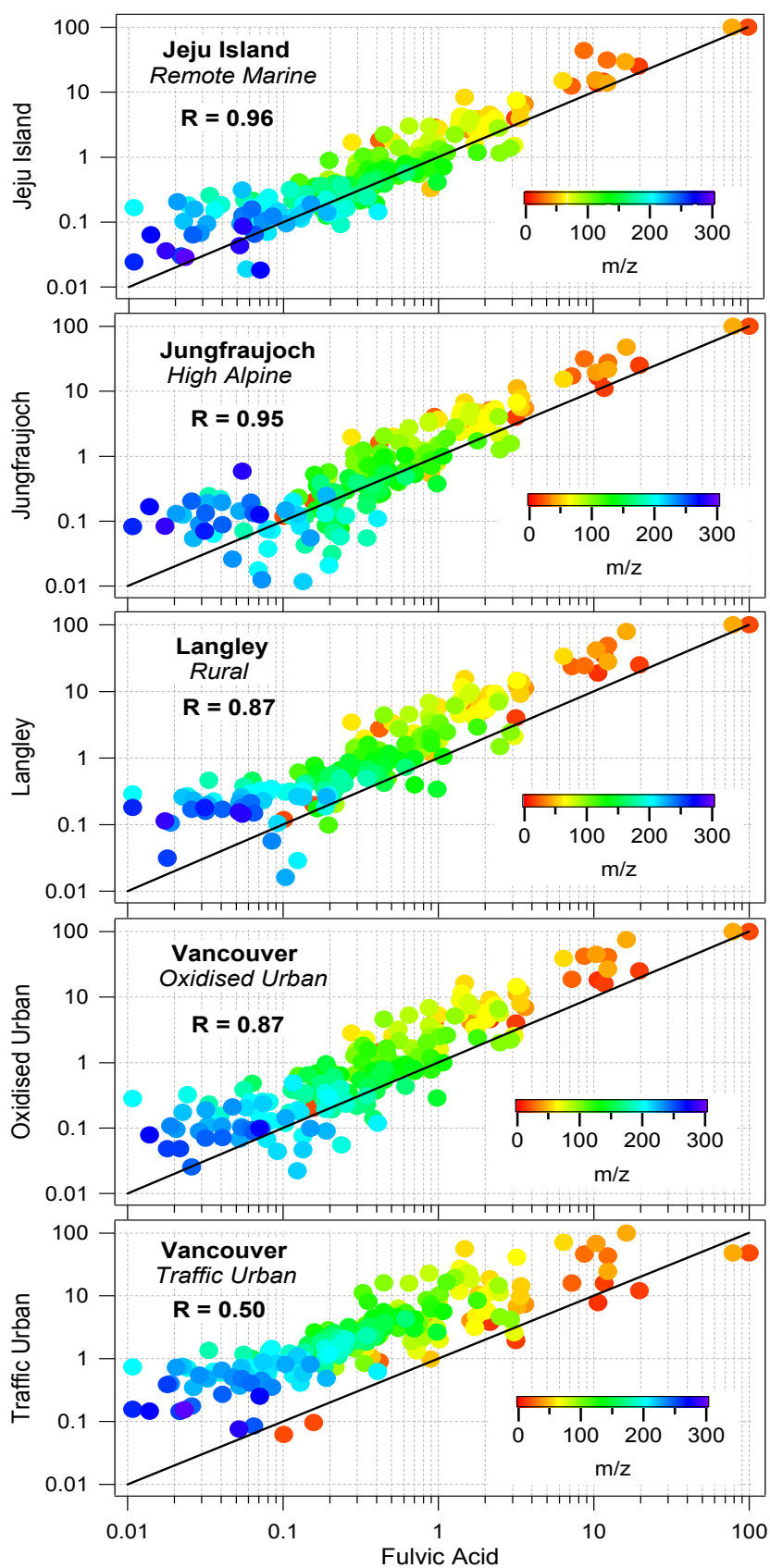
Figure 5.16: Scatter plots of organic mass spectra measured at various urban and non-urban locations against laboratory-generated fulvic acid spectrum. Data points are coloured according to their m/z value.

The contributions of mass fragments 44 and 57 to the total organic mass produced from the various sources and sampling locations described in this chapter are summarised in Figure 5.17. The degree of oxidation of the aerosol organic fraction ranged between the laboratory-generated diesel fuel and lubricating oil and fulvic acid as two extremes of primary and oxygenated organic carbon sources. Ambient data ranged from traffic dominated organic particulate to processed organics measured at remote sites in Jeju Island and the Swiss Alps (as has been discussed).
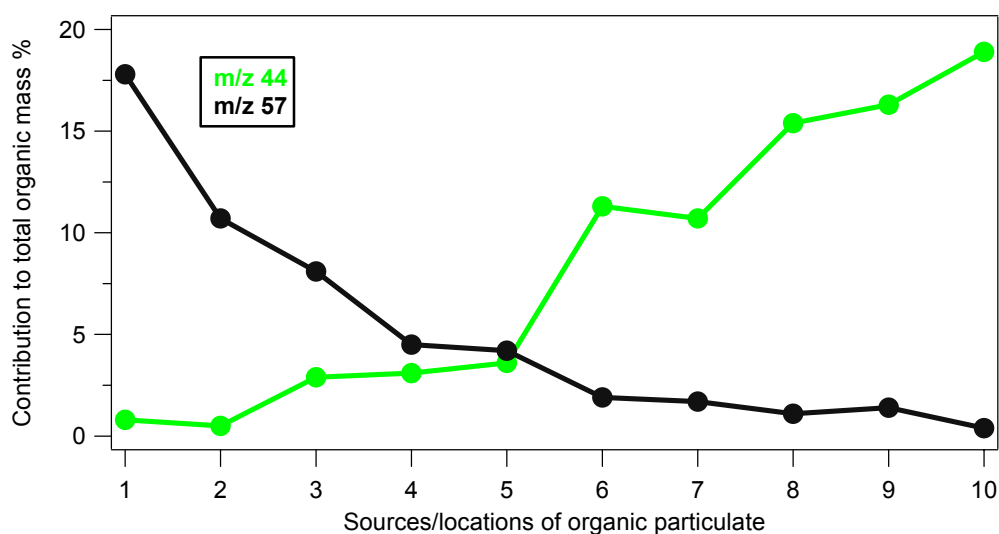

Figure 5.17: 1. Diesel fuel 2. Lubricating oil, 3. Diesel exhaust aerosol, 4. Traffic urban (UK) 5. Traffic urban(Canada) 6. Oxidised urban (Canada) 7. Rural (Canada) 8. high alpine (Jungfraujoch) 9. Remote marine, (Jeju Island) 10. Fulvic Acid

The results in Figure 5.17 strongly support the use of those two mass fragments as the AMS markers for oxygenated (*m/z 44*) and primary (*m/z 57*) organic carbon, as they clearly show that the contribution of *m/z* 44 to total organic mass increases from less than 1% in the case of diesel fuel and lubricating oil to about 19% in the fulvic acid case. On the contrary, *m/z* 57 contributed about 18% to the total organic mass in the diesel fuel sample and less than 1% in the fulvic acid case. A ratio of 44/57 less than 1 has been found for the diesel fuel and lubricating oil, diesel exhaust, as well as all the traffic dominated ambient particulate measured in Manchester winter and Vancouver, whereas, this ratio was found greater than 10 for the oxidised urban, rural and remote sites. These results may form the basis for future work to quantitatively classify the AMS organic data into fresh and oxygenated components using, respectively, *m/z* 57 and 44 as markers.

5.7 Summary

Chemical composition and mass size distribution results obtained using the Aerodyne Aerosol Mass Spectrometers (AMS) at various locations representing urban and regional settings around the world have been presented. A significant accumulation mode with a peak around 400 – 500 nm was observed at all locations and was composed of sulphate, organics, ammonium and nitrate. A significant organic mass mode at about 100 – 200 nm was constantly observed at all urban sites and when more freshly polluted air masses affected the other sites. The variability of the organic particulate composition and size distribution as a function of location and photochemical activity has been discussed. The small organic mode at the urban sites was found to be highly correlated with gas phase NO_x in Manchester and with CO, 1,3-butadiene, benzene and toluene in Vancouver with Pearson's r values of 0.86, 0.76, 0.71, 0.79 and 0.69, respectively. These correlation results suggest that combustion-related emissions (likely dominated by traffic) are the main source of the small organic mode at these sites. The chemical composition of organic aerosol at urban locations appeared to be very similar to the composition of lubricating oil and diesel exhaust aerosol, and contained a mixture of n-alkanes, branched alkanes, cycloalkanes, and aromatics. These results indicate that the organic fraction of urban aerosols is mostly dominated by the recondensed vapor from evaporated engine lubricating oil. These findings are similar to conclusions made in other studies that under most operating conditions the organic carbon fraction of in-use diesel vehicle exhaust aerosol is dominated by the recondensed vapor from the evaporated engine lubricating oil [*Tobias et al., 2001; Sakurai et al., 2003*]. Organics in the accumulation mode at the urban locations appeared to be composed of compounds of highly oxidised nature. This mode was significantly enhanced and dominated the organic mass size distribution during an episode of intensive photochemistry at the start of the study at the Slocan Park urban site in Vancouver.

In contrast to the urban sites, organic aerosols at all the other sites appeared to be dominated by oxidised compounds with shorter carbon chains. The mass spectral signatures at all of these locations were found to be very similar and the most significant contributions to these spectra arise from mass fragments characteristic of oxidised

organic compounds such as *m/z* 44 in addition to mass fragments 43 and 55. Correlations between the two organic modes and gas phase compounds at Langley indicated that a significant part of the small mode originated from combustion sources, while the large accumulation organic mode appeared to be the result of photochemical processing. Processing of organic particulate during a relatively high O_3 episode at Langley seemed to have increased the modal diameter of the accumulation mode from about 400 nm to 600 nm and almost doubled its mass loading. The mass spectral signatures of processed organic aerosols at various locations were found to be similar to that of fulvic acid. The latter is a model compound for humic-like substances; a group of highly oxidised organic compounds that have recently been found to contribute 20 – 50% to the water-soluble fraction of organic aerosol at urban and rural sites in Europe.